Limnol. Oceanogr., 50(5), 2005, 1438–1446

Maximum photosynthetic efficiency of size-fractionated phytoplankton assessed by ^{14}C uptake and fast repetition rate fluorometry

Pedro Cermeño[1] *and Patricia Estévez-Blanco*
Departamento de Ecología y Biología Animal, Facultad de Ciencias del Mar, Universidad de Vigo, 36310 Vigo, Spain

Emilio Marañón
Departamento de Ecología y Biología Animal, Facultad de Ciencias del Mar, Universidad de Vigo, 36310 Vigo, Spain; Laboratoire d'Océanographie de Villefranche, Centre National de la Recherche Scientifique, Universite Pierre et Marie Curie, 06234 Villefranche-sur-Mer, France

Emilio Fernández
Departamento de Ecología y Biología Animal, Facultad de Ciencias del Mar, Universidad de Vigo, 36310 Vigo, Spain

Abstract

Under high nutrient concentrations and sufficient light conditions, large phytoplankton may display higher photosynthetic efficiency than smaller cells. This is unexpected since smaller phytoplankton, because of their higher surface to volume ratio, possess a greater ability to take up nutrients and absorb light. In order to investigate the causes of the increased photosynthetic efficiency in larger phytoplankton, we assessed the maximum photosynthetic efficiency of coastal assemblages in three size classes (<5, 5–20, and >20 μm) by concurrently conducting ^{14}C-based photosynthesis–irradiance experiments and fast repetition rate fluorescence measurements. The light-saturated, chlorophyll-specific photosynthesis (P^b_{max}) and the maximum photosystem II (PSII) photochemical efficiency (F_v/F_m) of each size class were determined during winter mixing (March 2003) and summer stratification (June 2003). During winter mixing, size-fractionated P^b_{max} and F_v/F_m were similar in all size classes. In contrast, during summer stratification, size-fractionated P^b_{max} and F_v/F_m were significantly higher in the >20-μm size class. In the entire data set, size-fractionated P^b_{max} and F_v/F_m were not significantly correlated. However, a significant relationship was found between size-fractionated P^b_{max} and F_v/F_m for phytoplankton assemblages acclimated to low light conditions. Under high light, an excess PSII capacity may be responsible for the discrepancy between size-fractionated P^b_{max} and F_v/F_m measurements, whereas under low light conditions, photosynthetic electron transport chain and components downstream of PSII become more balanced, which results in a tight covariation between both variables. Higher maximum photosynthetic efficiencies of large-sized phytoplankton might be associated with a higher PSII photochemical efficiency characteristic of certain taxonomic groups such as diatoms.

Phytoplankton size structure plays a crucial role in controlling the trophic and biogeochemical functioning of pelagic ecosystems. Numerous field observations indicate that large-sized phytoplankton form the bulk of phytoplankton biomass in highly productive ecosystems, whereas smaller cells tend to dominate in unproductive regions of the ocean (Chisholm 1992). However, despite this well-established pattern, relatively little information is available on the physiological characteristics of different phytoplankton size classes in natural conditions, and thus the underlying causes for their distribution and dynamic behavior remain uncertain.

Traditionally, plankton physiologists have thought that small-sized phytoplankton possess energetic advantages due to their high surface to volume ratio, which results in a higher affinity for nutrients and a reduced package effect (Kiørboe 1993; Raven 1998). However, numerous reports indicate that, under favorable conditions for growth, large-sized phytoplankton can attain higher chlorophyll *a* (Chl *a*)–normalized photosynthetic rates than smaller phytoplankton (Legendre et al. 1993; Tamigneaux et al. 1999; Cermeño et al. 2005). In principle, these results suggest that under certain conditions large-sized phytoplankton may have a physiological advantage over smaller cells. However, Chl *a*–normalized photosynthetic rates are difficult to interpret because they depend on the cellular carbon to Chl *a* ratio, which is known to vary as a function of growth irradiance, nutrient status, taxonomic composition, or cell size. Furthermore, recent studies emphasize the need for interpreting photosynthesis–irradiance (P-E) experiments in the context of carbon-specific photosynthetic rates because under light-saturated conditions photosynthesis is not dependent on light absorption processes but on the efficiency of the photosynthetic electron transfer components [i.e., photosynthetic units] and the activity of Calvin-cycle enzymes (MacIntyre et al. 2002). Unfortunately, carbon biomass estimates in natural samples are subjected to different methodological shortcomings as-

[1] Corresponding author (pca@uvigo.es).

Acknowledgments

We thank D. Suggett and F. G. Figueiras for their insightful comments, which significantly improved an earlier version of the manuscript. We also thank S. Laney for his assistance in the processing of FRRF data and C. G. Castro for nutrient analyses. Two anonymous reviewers provided valuable comments. P.C. and P.E.-B. were supported by postgraduate research fellowships from the Spanish Ministerio de Ciencia y Tecnología (MCYT). This research was funded by MCYT and Xunta de Galicia through research grants REN2000-1248 and PXIC30102PN to E.M.

sociated with cell counting, calculation of biovolume, and the use of volume to carbon conversion factors. In addition, the photosynthetic parameters derived from P-E experiments, light-limited slope at low light intensities (α^b), and maximum Chl *a*–specific photosynthetic rate at saturating irradiances (P^b_{max}) provide an empirical description of photosynthetic efficiency but do not account for the underlying (physiological) mechanisms responsible for their variability (*see* Behrenfeld et al. 2004).

Fast repetition rate (FRR) fluorometry provides a measure of photosynthetic efficiency that is specific to photosystem II (PSII) photochemistry (Kolber et al. 1998). Specifically, fluorescence is measured following the progressive closure of PSII reaction centers by a series of subsaturating flashlets. Both light absorption and the number of reaction centers available for photochemistry modify the fluorescence that is observed (Falkowski and Raven 1997; Suggett et al. 2004). An initial fluorescence level, termed F_0, is obtained from the first flashlet when all reaction centers are open. In contrast, a maximum fluorescence level, termed F_m, is obtained once the majority of reaction centers are transporting electrons and temporarily closed to further excitation. Variable fluorescence ($F_v = F_m - F_0$) is scaled to the maximum fluorescence to yield the photochemical conversion efficiency of PSII, F_v/F_m (Butler 1978).

Previous research has demonstrated that F_v/F_m is related to $^{14}CO_2$ fixation or O_2 evolution in natural assemblages of phytoplankton (Boyd et al. 1997; Behrenfeld et al. 1998; Suggett et al. 2001). However, these studies did not investigate whether this relationship applies to all phytoplankton size classes or taxa within the photoautotrophic community. The FRR fluorescence technique has been applied to different size fractions in order to determine the effect of iron addition on the PSII photochemistry of phytoplankton in high nutrient–low chlorophyll regions (Kolber et al. 1994; Boyd and Abraham 2001). These researchers, however, did not investigate whether there were any significant differences in the photosynthetic response of each size fraction. Here we report on the maximum photosynthetic efficiency of three phytoplankton size classes (<5, 5–20, and >20 μm) as assessed from concurrent ^{14}C-uptake P-E experiments and FRR fluorescence measurements. We conducted our measurements during two contrasting hydrographic situations in a coastal embayment (Ría de Vigo, northwest Iberian Peninsula) characterized by intense horizontal, wind-driven circulation (Álvarez-Salgado et al. 2001) and a highly variable phytoplankton size structure (Tilstone et al. 1999). The concurrent determination of P-E parameters and F_v/F_m in different phytoplankton size classes allowed us to determine whether a noninvasive, fluorescence-based approach confirmed earlier, ^{14}C-based evidence that photosynthetic efficiency in natural phytoplankton assemblages may increase with cell size. (Cermeño et al. 2005). Our observations are discussed in the context of the underlying physiological mechanisms operating under natural, light-limiting, and light-saturating conditions.

Methods

We conducted eight visits to a station located in the central part of the Ría de Vigo (Fig. 1), a eutrophic coastal embayment where the depth of the water column is 45 m and the tidal range is about 2.5 m. Sampling was performed in two 2-week sampling periods during March and June 2003. Typically, sampling was completed between 0900 and 1000 h. On each visit, we recorded vertical profiles (0–40 m) of temperature with a Sea Bird Electronics SBE 39 conductivity, temperature, depth (CTD) probe. The vertical distribution of photosynthetically active irradiance (PAR, 400–700 nm) was measured with a spherical quantum sensor connected to a LiCor data logger. Seawater samples were collected from 0-, 5-, 10-, 15-, and 20-m depths in single 5-liter Niskin bottles. Special care was taken to prevent phytoplankton populations from light shock and temperature variability. Samples for the analysis of dissolved inorganic nutrients (nitrate, nitrite, ammonium, phosphate, and silicate) were immediately frozen and stored at −20°C until they were analyzed in the laboratory. A subsample (100 ml) was fixed with Lugol's solution (1% v/v) and stored in darkness until further microscopic analysis. Phytoplankton cells were identified with an inverted microscope following Uthermol's sedimentation technique. For the determination of size-fractionated Chl *a* concentration, two 250-ml replicates were filtered sequentially through 20-, 5-, and 0.2-μm polycarbonate filters, using low vacuum pressure (<100 mm Hg). Pigment was extracted by placing the filters in 90% acetone overnight. Chl *a* concentration was determined fluorometrically using a TD-700 fluorometer that had been calibrated with pure Chl *a* (Sigma).

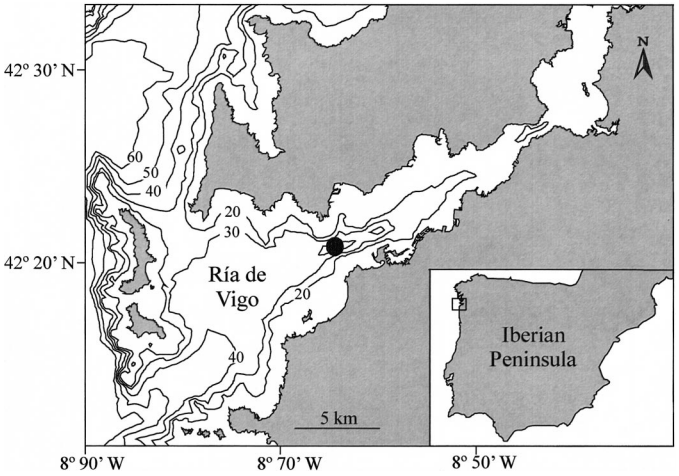

Fig. 1. Map of the study area (Ría de Vigo, northwest Iberian Peninsula) showing the sampling site.

A total of 16 size-fractionated (>20, 5–20, and <5 μm) P-E experiments were carried out using the ^{14}C-uptake technique on samples collected at surface and 15-m depth. We used bench incubators equipped with 100 W halogen lamps and cooled by running water passing through a refrigerator, which maintained samples within 0.5°C of the in situ temperature. Each incubator held 13 samples that were exposed to an irradiance gradient from 5 to 2,000 μmol m^{-2} s^{-1}. Light was attenuated by neutral density filters and the incubation bottles. Irradiance at each position of the incubator was measured each day before incubation using a LiCor quantum sensor. Seawater samples were dispensed into 70-ml poly-

styrene bottles that were inoculated with 370 kBq (10 μCi) of $NaH^{14}CO_3$ and incubated for 2 h. For each experiment, one bottle was wrapped with aluminum foil prior to incubation and the corresponding dark disintegrations per minute (DPM) value was subsequently subtracted from the ^{14}C activity of each light sample. At the end of the incubation, samples were filtered sequentially through 20-, 5-, and 0.2-μm polycarbonate filters under low vacuum pressure (<100 mm Hg). Inorganic carbon on the filters was removed by exposing them to concentrated HCl fumes overnight. After decontamination, filters were placed into scintillation vials to which 4 ml of scintillation cocktail was added. Radioactivity was measured on a 1409-012 Wallac scintillation counter that used an internal standard for quenching correction.

The results of each P-E experiment were fitted to the model of Webb et al. (1974) since no photoinhibition was observed:

$$P_z^b = P_{\max}^b \left[1 - \exp\left(-\frac{\alpha^b E}{P_{\max}^b}\right)\right]$$

where P_z^b [mg C mg Chl a^{-1} h^{-1}] is the Chl *a*–normalized rate of C incorporation, $P_{\max}^b$ [mg C mg Chl a^{-1} h^{-1}] is the maximum light-saturated rate of Chl *a*–normalized C incorporation, α^b [mg C mg Chl a^{-1} h^{-1} (μmol m^{-2} s^{-1})$^{-1}$] is the initial slope of the P-E curve, and E is the irradiance (μmol m^{-2} s^{-1}). The irradiance saturating parameter (I_K) was determined as $P_{\max}^b/\alpha^b$.

FRR fluorescence measurements were made using a Chelsea Instruments Fast^{tracka} FRR fluorometer (serial no. 182045). The instrument was programmed with a single-turnover protocol that provides a flash sequence consisting of a series of 100 saturation flashlets (1.34 μs flash duration and 2.8 μs flash period) and a series of 20 relaxation flashlets (1.34 μs flash duration and 51.6 μs flash period). FRR fluorescence measurements were initially made on unfractionated (total) water samples collected from the surface and from 15-m depth. Samples were dark adapted for 30 min to allow relaxation of nonphotochemical quenching (Babin et al. 1996). Each sample was then placed into the FRR fluorometer dark chamber and 25 acquisitions of 8 averaged flash sequences were made in autogaining mode. Triplicates were measured for each sample. These FRR fluorescence measurements were also repeated on size-fractionated water samples. An aliquot of 250 ml was filtered by gravity through 20- and 5-μm polycarbonate filters and then gently resuspended in 100 ml of the original seawater sample filtered through Millipore APFF glass-fiber filters. This procedure allowed us to obtain the >20- and 5–20-μm size classes. The <5-μm size class was obtained by collecting the filtrate after filtration of the whole sample through 20- and 5-μm polycarbonate filters. Three subsamples of each size fraction were measured as above. Blanks for each depth were obtained by filtering the original seawater sample through Millipore APFF glass-fiber filters (Cullen and Davis 2003). FRR fluorescence from the filtrates was measured at fixed gain settings and subtracted from the sample values. An additional experiment was carried out in order to determine whether blanks from total and size-fractionated samples showed any significant difference. After size fractionation of a natural seawater sample, the three replicates of total and size-fractionated samples were dark adapted for 30 min and filtered separately through Millipore APFF glass-fiber filters. FRR fluorescence of all blanks was measured, and statistical analysis indicated no significant differences between total and size-fractionated blanks (Kruskal–Wallis test, $p > 0.05$). Thus, we had complete confidence in using a single blank from the total sample for all size-fractionated FRR fluorescence measurements.

Fluorescence variables F_0 (initial fluorescence), F_m (maximal fluorescence), and σ_{PSII} (the functional absorption cross section of photosystem II) were obtained by fitting the model of Kolber et al. (1998) to the FRR fluorescence using v5 codes (S. Laney) run in Matlab. All acquisitions for each sample were averaged into single excitation/emission files to reduce the variability of the data prior to processing. Fluorescence transients were corrected for nonlinearities in the instrument response (Laney 2003). FRR fluorescence measurements were carried out with different gain settings depending on the amount of chlorophyll of each sample.

Results

Hydrography and phytoplankton distribution—In March 2003, the water column was characterized by vertical mixing. During this period, seawater temperature ranged from 12.7°C to 14.2°C (Fig. 2). We measured high concentrations of dissolved inorganic nitrogen (DIN) (>4.5 μmol L^{-1}), phosphate (>0.15 μmol L^{-1}), and silicate (>3.5 μmol L^{-1}) throughout the water column. At the surface, Chl *a* varied from 1.5 to 10 mg m^{-3}, whereas in depth, Chl *a* concentrations never exceeded 4.5 mg m^{-3} (Fig. 2). On average, <5-, 5–20-, and >20-μm size fractions accounted for (mean ± 1 standard deviation) 46% ± 9%, 27% ± 5% and 27% ± 8% of total euphotic layer–integrated Chl *a*, respectively (Fig. 3).

In June 2003, typical summer stratification prevailed. The thermocline was located at around 5-m depth. Temperature decreased from 17°C to 19°C at the surface to 14°C at 15 m depth (Fig. 2). During this period, DIN concentrations were in the range 0.2–2.1 μmol L^{-1} at the surface and 0.9–9.4 μmol L^{-1} at 15 m. At the surface, phosphate and silicate concentrations were in the range 0.04–0.2 and 0.1–1 μmol L^{-1}, respectively, whereas higher concentrations were measured near the bottom of the photic layer. Figueiras and Pazos (1991) observed that summer stratification is generally characterized by the accumulation of phytoplankton in the vicinity of the thermocline. They associated this observation with a positive estuarine circulation that provides nutrients to the euphotic layer and maintains actively growing phytoplankton assemblages close to the thermocline. During this period, total Chl *a* exceeded 3.9 mg m^{-3} at 15 m, whereas in the surface, total Chl *a* ranged from 1.5 to 5 mg m^{-3} (Fig. 2). On average, microphytoplankton size class accounted for more than 70% of total euphotic layer–integrated Chl *a* in June 2003 (Fig. 3). This pattern in the size-fractionated Chl *a* was consistent throughout the water column.

Marked differences were observed in the composition of microbial plankton between March and June (Table 1). Cryp-

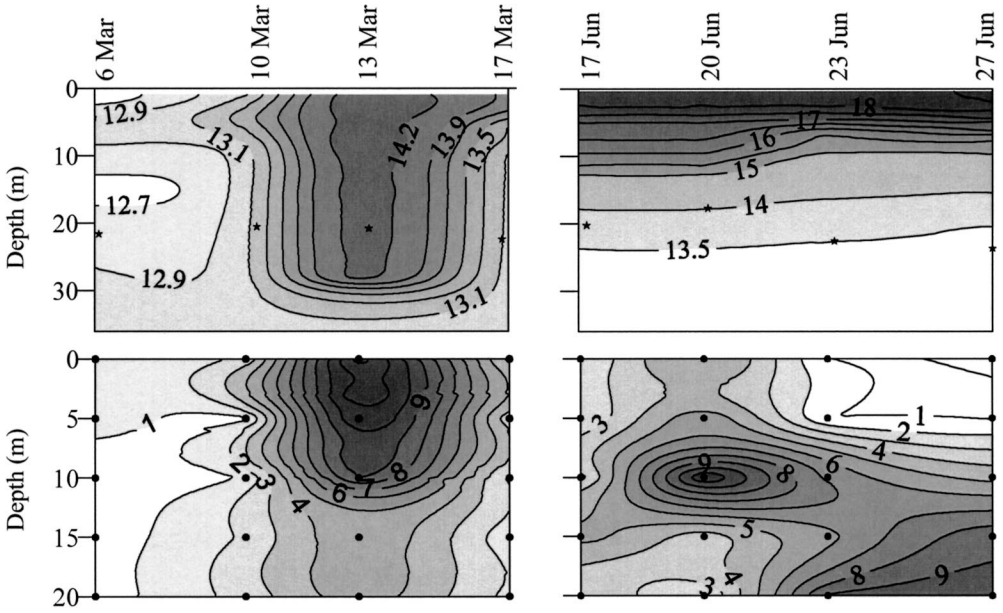

Fig. 2. Evolution of temperature (°C, upper panels) and Chl *a* concentration (mg m^{-3}, lower panels) in the Ría de Vigo during March and June 2003. Symbols in temperature plots indicate depth of the euphotic layer (1% optical depth).

tophyceans and small unidentified flagellates dominated the microbial plankton community in March. In June, while small unidentified flagellates were still present in similar numbers, diatoms and dinoflagellates significantly increased their abundances. For instance, the chain-forming genus *Chaetoceros* reached abundances as high as 460,000 cells L^{-1}. These differences in the composition of the microbial plankton community were clearly reflected in the changes in size-fractionated Chl *a* concentration (Fig. 3).

Phytoplankton photophysiology—Figure 4 shows four representative size-fractionated, P-E relationships obtained during each sampling period at surface and depth. In March, the mean (±1 standard deviation) P^b_{max} for the whole phytoplankton assemblage differed markedly between the surface (4.9 ± 1.4 mg C mg Chl a^{-1} h^{-1}) and 15 m (2.2 ± 1.1 mg C mg Chl a^{-1} h^{-1}). Mean surface P^b_{max} values were 4.4 ± 1.1 for the <20-μm size class and took higher values (5.8 ± 1.7) for the >20-μm size class (Fig. 5). However, statistical analyses did not reveal significant differences in P^b_{max} between size classes (Kruskal–Wallis test, $p > 0.05$). In June, whole phytoplankton P^b_{max} was 7.9 ± 0.7 at the surface and 2.8 ± 0.4 at 15 m. In contrast to the observations from March, P^b_{max} showed important differences between size classes during June. Surface P^b_{max} was 8.7 ± 1.1, 5.6 ± 1.3, and 4.3 ± 1.2 for the >20-, 5–20-, and <5-μm size classes, respectively (Fig. 5). P^b_{max} at 15 m was 3.1 ± 0.4, 1.8 ± 0.2, and 1.8 ± 0.1 for the three size classes. For both depths, a Mann–Whitney test ($p < 0.05$) indicated that P^b_{max} for the >20-μm size fraction was significantly higher than those from the smaller fractions.

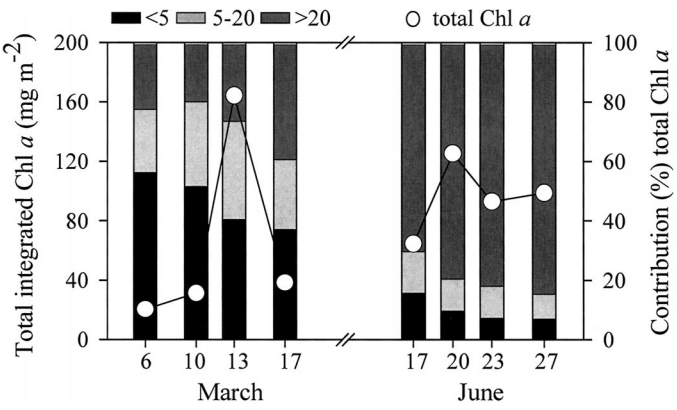

Fig. 3. Total euphotic layer–integrated Chl *a* concentration (line and open circles) and contribution (%) of each size fraction to total Chl *a* (bars) during March and June 2003.

I_K values during March varied between 125 and 325 μmol photon m^{-2} s^{-1} (Fig. 6). No statistical differences were observed between surface and 15-m samples (Mann–Whitney test, $p > 0.05$), which strongly suggests that vertical mixing was preventing phytoplankton from acclimating to low irradiance deep in the water column. Thus, during this sampling period phytoplankton cells were likely to experience highly variable light regimes. In contrast, I_K values during June were much higher at surface than at 15-m depth (100–250 vs. 20–100 μmol photon m^{-2} s^{-1}, *see Fig. 6*). These differences were highly significant (Mann–Whitney test, $p < 0.001$) and suggest that phytoplankton cells living in deep waters were acclimated to low irradiance levels as a result of the persistent stratification of the water column.

F_v/F_m from unfractionated samples ranged from 0.44 to 0.53 throughout March and June. In March, the mean F_v/F_m from unfractionated samples was 0.47 ± 0.02 at the surface and 0.48 ± 0.03 at 15 m. Surface values of F_v/F_m from the <5-, 5–20-, and >20-μm size classes were 0.44 ± 0.03,

Table 1. Abundance (cells ml^{-1}) of the most frequent microbial plankton taxonomic categories during the sampling period.

	6 Mar 03		13 Mar 03		17 Jun 03		23 Jun 03	
Phytoplankton species	0 m	15 m	0 m	15 m	0 m	15 m	0 m	15 m
Chaetoceros spp.					460	60	363	18
Leptocylindrus danicus	0.04				3.1	2.6	0.2	17
Rhizosolenia alata					0.1	0.7	0.04	0.8
Rhizosolenia delicatula					0.7	0.5	0.24	11
Dinophysis acuminata					0.16	0.7	2.0	0.16
Gyrodinium spp.	0.04	0.28		0.16	0.48	1.3	0.16	0.12
Pyrocystis lunula					0.08	0.32	0.24	0.08
Scrippsiella trochoidea					0.04	0.16	0.08	2.2
Small unidentified flagellates	1,096	704	1,960	1,752	1,290	1,761	713	271
Cryptophyceans	672	125	2,416	310	27	70	28	27
Small ''naked'' dinoflagellates	9.1	2.6	86	5.2	41	32	14	22
Oligotrich ciliates	0.96	0.44	15	6.4	0.4	3.4	3.1	2.3

0.41 ± 0.09, and 0.48 ± 0.01, respectively (Fig. 7). Statistical analyses did not reveal significant differences in F_v/F_m between size classes (Kruskal–Wallis test, $p > 0.1$). In June, F_v/F_m from unfractionated samples was 0.52 ± 0.01 at surface and 0.47 ± 0.02 at 15 m. On this occasion, F_v/F_m showed marked differences between size classes. Surface F_v/F_m was 0.53 ± 0.01, 0.42 ± 0.04, and 0.49 ± 0.04 for the >20-, 5–20-, and <5-μm size classes, respectively (Fig. 7). F_v/F_m at 15 m was 0.46 ± 0.03, 0.37 ± 0.02, and 0.38 ± 0.03 for the three size classes. For both depths, a Mann–Whitney test ($p < 0.05$) indicated that F_v/F_m for the >20-μm size fraction was significantly higher than those from the smaller fractions.

It is conceivable that our methodological procedures, specifically the sample fractionation for measuring size-fractionated F_v/F_m, might have stressed phytoplankton cells, thus resulting in biased estimates. In order to verify this possibility, we estimated the total F_v/F_m from the sum of each size-fractionated value of F_v/F_m weighted by the Chl *a* biomass as follows:

$$\frac{F_v}{F_{m(\text{total})}} = \frac{\sum_{i=1}^{3} F_v/F_{m(i)}[\text{Chl } a_{(i)}]}{\sum \text{Chl } a_{(i)}}$$

where $F_v/F_{m(i)}$ and Chl $a_{(i)}$ are F_v/F_m and Chl *a* concentration for each size fraction (*i*). This approach is analogous to the one used by Suggett et al. (2004), who calculated total σ_{PSII} in mixed algal assemblages by summing the σ_{PSII} signatures of each size class, weighted by its fluorescence. Calculations of $F_v/F_{m(\text{total})}$ and $\sigma_{\text{PSII(total)}}$ from the size-fractionated samples were highly correlated ($r^2 > 0.78$, $p < 0.0001$) with F_v/F_m and σ_{PSII} measured from the unfractionated samples. In both cases, the intercept and slope of the linear fits were not significantly different from 0 and 1, respectively (*t*-test, $p > 0.05$). These results suggest that our size-fractionation procedures did not alter significantly the physiological state of phytoplankton cells and give us further reassurance on the validity of measuring FRR fluorescence with different gains depending on the concentration of Chl *a*.

Discussion

Potential mechanisms for size-related differences in photosynthetic efficiency—Our size-fractionated P-E experiments and F_v/F_m measurements indicated that during the June sampling period, large-sized phytoplankton had higher maximum photosynthetic efficiency than smaller phytoplankton. Laboratory investigations have shown that F_v/F_m is related to the maximum photosynthetic efficiency and, in turn, to the growth rate (Kolber and Falkowski 1988; Herzig and Falkowski 1989). Therefore, F_v/F_m displays distinct variability between taxa (Koblizek et al. 2001) and also depending on light and nutrient conditions (Kolber and Falkowski 1988; Herzig and Falkowski 1989), although there is insufficient evidence in the literature to strictly link these variations to phytoplankton size classes.

Our observations would appear to contradict both theoretical and experimental studies showing that small cells tend to have higher mass-specific photosynthetic rates as a result of their higher surface to volume ratio (Eppley and Sloan 1966; *see* Peters 1983 for a review). Similar contradictory evidence was reported by Banse (1982) and Furnas (1990). They observed that under sufficient resource conditions, namely, high irradiance and nutrient concentrations, diatoms grow faster than flagellates of the same size, but they did not provide any physiological mechanism to explain such differences. The higher maximum photosynthetic efficiency of large-sized phytoplankton cannot stem from an advantageous ability to absorb light because of their low surface to volume ratio and high pigment packaging. A similar reasoning may be applied for nutrient uptake. However, some studies have suggested that luxury uptake of nutrients by diatoms and their subsequent intracellular storage may allow the cells to sustain relatively high growth rates even when nutrients in the environment are depleted (Geider et al. 1986; Raven 1997). Previous analysis using flow cytometry and microscopy image analysis during a full annual cycle in the Ría de Vigo (Cermeño et al. 2005) indicates that there exists an important degree of variability in the taxonomic composition across the size spectrum, from small cyanobacteria and picoeukaryotes to large dinoflagellates and diatoms. This rais-

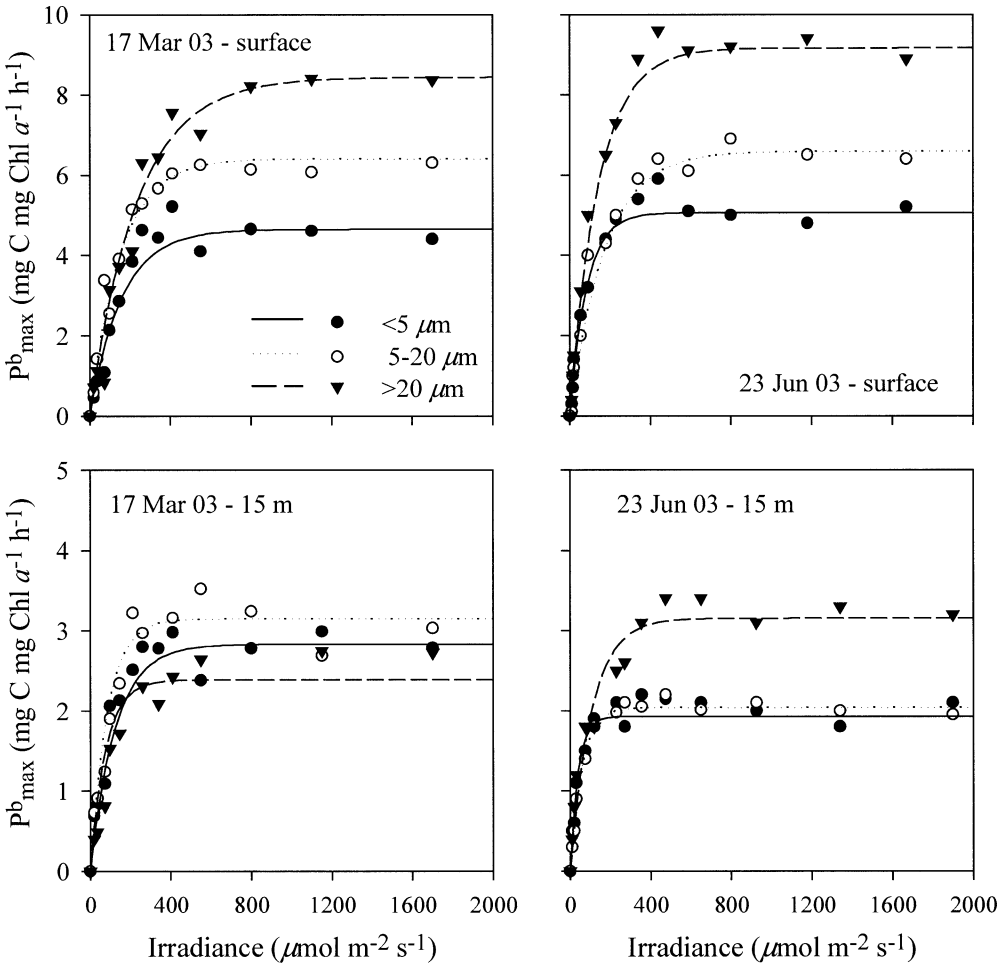

Fig. 4. Representative size-fractionated photosynthesis–irradiance relationships of phytoplankton from the surface and 15-m depth in March and June 2003.

es the possibility that the observed differences in photosynthetic efficiency between size classes may reflect taxon-related differences in photophysiology rather than the effect of cell size.

There is some previous evidence for taxon-related differences in F_v/F_m. Some groups such as cyanobacteria typically have very low F_v/F_m (Koblizek et al. 2001). However, this is partially due to the presence of phycocyanin, whose fluorescence spectrum partially overlaps with that of other pigments such as Chl *a* (Campbell et al. 1998; Suggett et al. 2004). Other studies have investigated the variability of F_v/F_m between size classes, and potentially taxa, in high nutrient–low chlorophyll regions during iron-enrichment experiments (Kolber et al. 1994; Boyd and Abraham 2001). These analyses showed that after iron addition all size fractions displayed a significant increase in F_v/F_m, highlighting the effect of iron limitation on the activity of PSII. Furthermore, Boyd and Abraham (2001) reported higher F_v/F_m values in the >20-μm size fraction, mainly composed by chain-forming diatoms, than in the smaller size fractions. Our analysis of size-fractionated $P^b_{\max}$ and F_v/F_m is consistent with this observation and adds further evidence to conclude that, under favorable conditions for growth, large-sized phytoplankton, and diatoms in particular, may have higher photosynthetic efficiencies than smaller cells.

Relation between P^b_{max}, F_v/F_m, *and phytoplankton photoacclimation*—It is well accepted that, under low irradiance conditions, photosynthesis is limited by the rate at which photons are absorbed by the light-harvesting complexes. As irradiance increases, more photosynthetic units, including both photosystems I and II (PSI and PSII), become progressively occupied (active) and C assimilation increases linearly. Some cycling of electrons around PSI may be required to maintain ATP synthesis under low light conditions (Falkowski and Raven 1997). Once the saturating irradiance is reached, light absorption exceeds its use rate and C assimilation is limited by the secondary photosynthetic reactions such as the efficiency of the photosynthetic electron transfer components, the enzymatic activity of the Calvin-cycle components (Sukenik et al. 1987; Falkowski and Raven 1997; Behrenfeld et al. 2004), or the ability of nonphotochemical pathways to prevent damage via overexcitation of reaction centers (MacIntyre et al. 2002). Photosynthetic parameters, α^b in the initial region of the P-E curve, and $P^b_{\max}$ in the saturating irradiance region, provide an empirical description

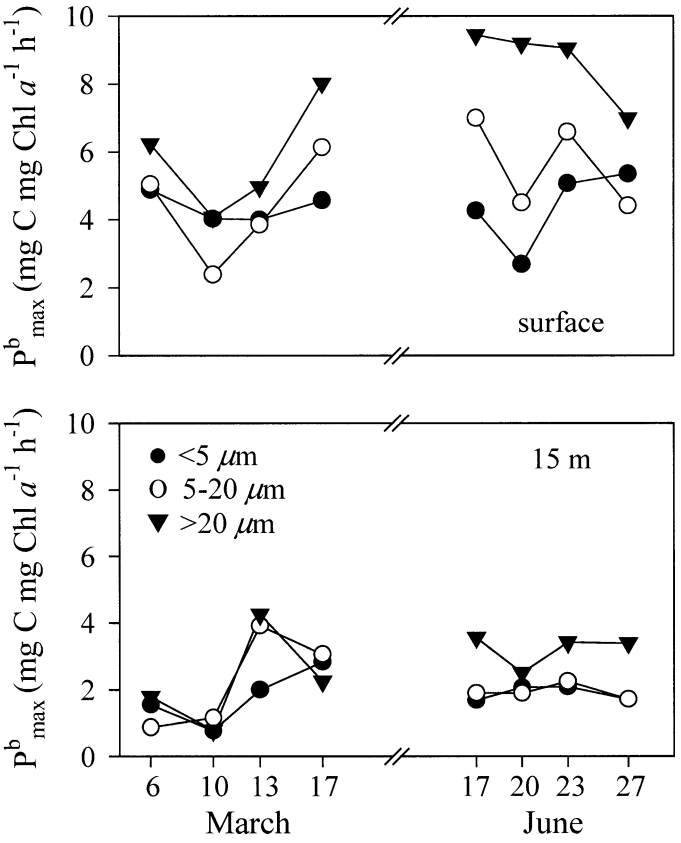

Fig. 5. Size-fractionated P^b_{max} in March and June 2003. Upper panel is for surface samples and lower panel for samples collected at 15-m depth.

of these processes but do not account for the physiological mechanisms involved in their variability.

As stated above, P^b_{max} may be governed by processes remote from PSII photochemistry, such as the activity of the Calvin-cycle enzymes (Falkowski and Raven 1997). According to this, our attempt to relate P^b_{max} andF_v/F_m did not show any clear relationship for the entire data set, ($r^2 = 0.14$, $n = 39$, $p = 0.02$) (Fig. 8A). Recent studies have suggested that phytoplankton acclimated to high (surface) or variable (upper mixed layer) light conditions tend to develop an excess PSII capacity as a strategy against reaction center damage from increased light levels (Behrenfeld et al. 1998; Kaňa et al. 2002). This mechanism obstructs any relationship between P^b_{max} and F_v/F_m because the excess capacity of PSII limits maximum photosynthesis by components downstream of PSII. At lower irradiances, however, the possibility of photodamage to PSII is reduced and photosynthetic electron transport chain and downstream components may become more balanced (Genty and Harbinson 1996).

Following the theoretical basis above, we investigated the relationship between P^b_{max} and F_v/F_m for those samples acclimated to low irradiances, in particular those corresponding to subsurface levels during the summer stratification, which showed significantly lower I_k values than surface samples (Fig. 6). In this case, a highly significant relationship ($r^2 = 0.81$, $n = 12$, $p < 0.0001$) was found, suggesting that under these environmental conditions the maximum photosynthetic

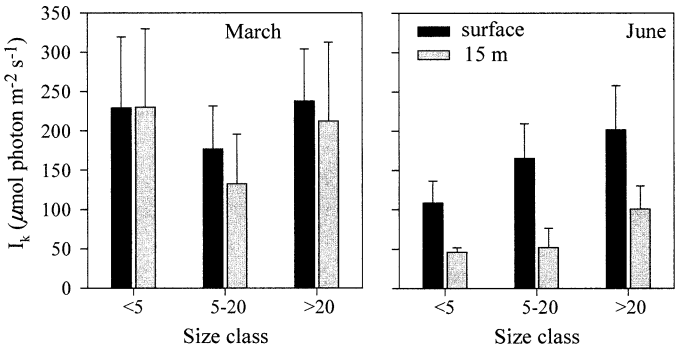

Fig. 6. Averaged I_K values in March and June 2003. Error bars indicate ±1 standard deviation.

efficiency can be related to changes in F_v/F_m (Fig. 8B). Thus, in spite of the geometrical advantages of smaller cells for nutrient uptake and light absorption, large-sized phytoplankton may possess photophysiological advantages over smaller cells, mainly related to an enhanced photochemical efficiency of PSII.

In summary, two measures of photosynthetic efficiency, P^b_{max} and F_v/F_m, in different size fractions show that large-sized phytoplankton may have higher photosynthetic efficiency than smaller cells. However, these parameters cannot be directly related since they account for different processes.

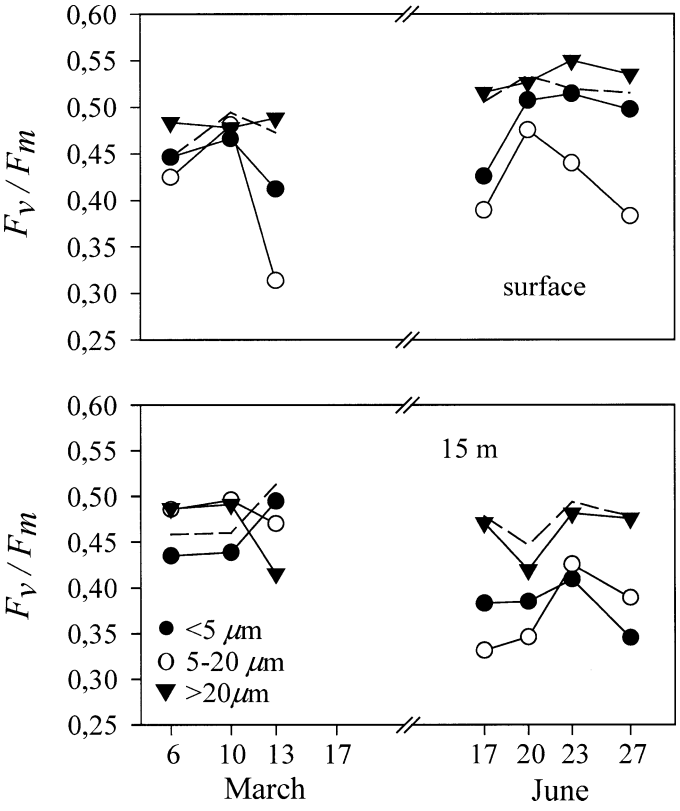

Fig. 7. Size-fractionated F_v/F_m in March and June 2003. Upper panel is for surface samples and lower panel for samples collected at 15-m depth. Symbols are as in Fig. 2. Dashed lines represent F_v/F_m of total, unfractionated sample.

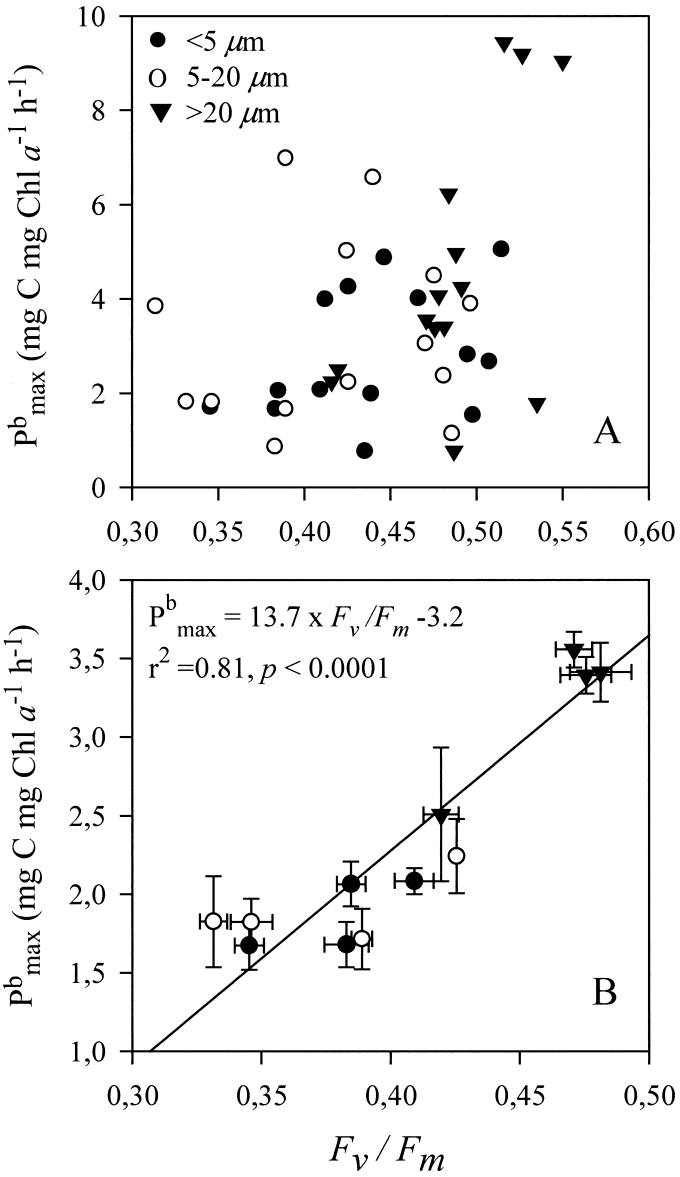

Fig. 8. Relationship between size-fractionated P^b_{max} and F_v/F_m using (A) the whole data set, and (B) 15-m-depth samples collected in June 2003. Solid line represents reduced major axis regression analysis.

P^b_{max} is an estimate of carbon assimilation per unit pigment content at light-saturating conditions. On the contrary, F_v/F_m is an estimate of the maximum photochemical efficiency of electron transport through PSII, and as such is more related to oxygen evolution than to carbon fixation. When pooled together, our data did not show any clear covariation between P^b_{max} and F_v/F_m. However, we found a highly significant relationship between both parameters for phytoplankton assemblages acclimated to low light levels. This covariation might be associated with a tighter connection between processes taking place in and downstream of PSII. Our results suggest that PSII photochemistry plays an important role in controlling the overall photosynthetic performance and provides a possible mechanism to account for the higher photosynthetic efficiency of larger phytoplankton under favorable conditions for growth.

References

Álvarez-Salgado, X. A., J. Gago, B. M. Míguez, and F. F. Pérez. 2001. Net ecosystem production of dissolved organic carbon in a coastal upwelling system: The Ría de Vigo, Iberian margin of the North Atlantic. Limnol. Oceanogr. **46:** 135–147.

Babin, M., A. Morel, H. Claustre, A. Bricaud, Z. Kolber, and P. G. Falkowski. 1996. Nitrogen and irradiance-dependent variations in the maximum quantum yield of carbon fixation in eutrophic, mesotrophic and oligotrophic marine systems. Deep-Sea Res. I Oceanogr. Res. Pap. **43:** 1241–1272.

Banse, K. 1982. Cell volumes, maximal growth rates of unicellular algae and ciliates, and the role of ciliates in the marine pelagial. Limnol. Oceanogr. **27:** 1059–1071.

Behrenfeld, M. J., O. Prasil, M. Babin, and F. Bruyant. 2004. In search of a physiological basis for covariations in light-limited and light-saturated photosynthesis. J. Phycol. **40:** 4–25.

———, ———, Z. S. Kolber, M. Babin, and P. G. Falkowski. 1998. Compensatory changes in Photosystem II electron turnover rates protect photosynthesis from photoinhibition. Photosynth. Res. **58:** 259–268.

Boyd, P. W., and E. R. Abraham. 2001. Iron-mediated changes in phytoplankton photosynthetic competence during SOIREE. Deep-Sea Res. II **48:** 2529–2550.

———, J. Aiken, and Z. Kolber. 1997. Comparison of radiocarbon and fluorescence based (pump and probe) measurements of phytoplankton photosynthetic characteristics in the Northeast Atlantic Ocean. Mar. Ecol. Prog. Ser. **419:** 215–226.

Butler, W. L. 1978. Energy distribution in the photochemical apparatus of photosynthesis. Annu. Rev. Plant Physiol. **29:** 345–378.

Campbell, D., V. Hurry, A. Clarke, P. Gustafsson, and G. Öquist. 1998. Chlorophyll fluorescence analysis of cyanobacterial photosynthesis and acclimation. Microbiol. Mol. Biol. Rev. **62:** 667–683.

Cermeño, P., E. Marañón, J. Rodríguez, and E. Fernández. 2005. Large-sized phytoplankton sustain higher carbon-specific photosynthesis than smaller cells in a coastal eutrophic ecosystem. Mar. Ecol. Prog. Ser. **297:** 51–60.

Chisholm, S. W. 1992. Phytoplankton size, p. 213–237. *In* P. G. Falkowski and A. D. Woodhead [eds.]. Primary productivity and biogeochemical cycles in the sea. Plenum.

Cullen, J. J., and R. F. Davis. 2003. The blank can make a big difference in oceanographic measurements. Limnol. Oceanogr. Bull. **12:** 29–35.

Eppley, R. W., and P. R. Sloan. 1966. Growth rates of marine phytoplankton: Correlation with light absorption by cell chlorophyll *a.* Physiol. Plant. **19:** 47–59.

Falkowski, P. G., and J. A. Raven. 1997. Aquatic photosynthesis. Blackwell.

Figueiras, F. G., and Y. Pazos. 1991. Microplankton assemblages in three Rías Baixas (Vigo, Arosa and Muros, Spain) with a subsurface chlorophyll maximum: Their relationships to hydrography. Mar. Ecol. Prog. Ser. **76:** 219–233.

Furnas, M. L. 1990. In situ growth rates of marine phytoplankton: Approaches to measurement, community and species growth rates. J. Plankton Res. **12:** 1117–1151.

Geider, R., T. Platt, and J. A. Raven. 1986. Size dependence of growth and photosynthesis in diatoms: A synthesis. Mar. Ecol. Prog. Ser. **30:** 93–104.

Genty, B., and J. Harbinson. 1996. Regulation of light utilization

for photosynthetic electron transport, p. 67–99. *In* N. Baker [ed.], Photosynthesis and the environment, v. 5. Kluwer.

HERZIG, R., AND P. G. FALKOWSKI. 1989. Nitrogen limitation of *Isochrysis galbana* (Haptophyceae). I. Photosynthetic energy conversion and growth efficiencies. J. Phycol. **25:** 462–471.

KAŇA, T., D. LAZAR, O. PRASIL, AND J. NAUS. 2002. Experimental and theoretical studies on the excess capacity of Photosystem II. Photosynth. Res. **72:** 271–284.

KIØRBOE, T. 1993. Turbulence, phytoplankton cell size and the structure of pelagic food webs. Adv. Mar. Biol. **29:** 1–72.

KOBLIZEK, M., D. KAFTAN, AND L. NEDBAL. 2001. On the relationship between the non-photochemical quenching of the chlorophyll fluorescence and the Photosystem II light harvesting efficiency. A repetitive flash fluorescence induction study. Photosynth. Res. **68:** 141–152.

KOLBER, Z., R. T. BARBER, K. H. COALE, S. E. FITZWATER, R. M. GREENE, K. S. JOHNSON, S. LINDLEY, AND P. G. FALKOWSKI. 1994. Iron limitation of phytoplankton photosynthesis in the Equatorial Pacific Ocean. Nature **371:** 145–149.

———, AND P. G. FALKOWSKI. 1988. Effects of growth irradiance and nitrogen limitation on photosynthetic energy conversion in Photosystem II. Plant Physiol. **88:** 72–79.

———, O. PRASIL, AND P. G. FALKOWSKI. 1998. Measurements of variable chlorophyll fluorescence using fast repetition rate techniques: Defining methodology and experimental protocols. Biochim. Biophys. Acta **1367:** 88–106.

LANEY, S. R. 2003. Assessing the error in photosynthetic properties determined by fast repetition rate fluorometry. Limnol. Oceanogr. **48:** 2234–2242.

LEGENDRE, L., M. GOSSELIN, HJ. HIRCHE, G. KATTNER, AND G. ROSENBERG. 1993. Environmental control and potential fate of size fractionated phytoplankton in the Greenland Sea (75°N). Mar. Ecol. Prog. Ser. **98:** 297–313.

MACINTYRE, H. L., T. M. KANA, T. ANNING, AND R. J. GEIDER. 2002. Photoacclimation of photosynthesis irradiance response curves and photosynthetic pigments in microalgae and cyanobacteria. J. Phycol. **38:** 17–38.

PETERS, R. H. 1983. The ecological implications of body size. Cambridge University Press. Cambridge.

RAVEN, J. A. 1997. The vacuole: A cost-benefit analysis. Adv. Bot. Res. **25:** 59–86.

———. 1998. Small is beautiful: The picophytoplankton. Funct. Ecol. **12:** 503–513.

SUGGETT, D. J., K. GIJSBERT, P. M. HOLLIGAN, M. DAVEY, J. AIKEN, AND R. GEIDER. 2001. Assessment of photosynthesis in a spring cyanobacterial bloom by use of a fast repetition rate fluorometer. Limnol. Oceanogr. **46:** 802–810.

———, H. L. MACINTYRE, AND R. J. GEIDER. 2004. Evaluation of biophysical and optical determinations of light absorption by photosystem II in phytoplankton. Limnol. Oceanogr. Methods **2:** 316–332.

SUKENIK, A., J. BENNET, AND P. G. FALKOWSKI. 1987. Light-saturated photosynthesis-limitation by electron transport or carbon-fixation? Biochim. Biophys. Acta **891:** 205–215.

TAMIGNEAUX, E., L. LEGENDRE, B. KLEIN, AND M. MINGELBIER. 1999. Seasonal dynamics and potential fate of size-fractionated phytoplankton in a temperate nearshore environment (Western Gulf of St. Lawrence, Canada). Estuar. Coast. Shelf Sci. **48:** 253–269.

TILSTONE, G. H., F. G. FIGUEIRAS, E. G. FERMIN, AND B. ARBONES. 1999. Significance of nanophytoplankton photosynthesis and primary production in a coastal upwelling system (Ría de Vigo, NW Spain). Mar. Ecol. Prog. Ser. **183:** 13–27.

WEBB, W. L. M., M. NEWTON, AND D. STARR. 1974. Carbon dioxide exchange of *Alnus rubra:* A mathematical model. Oecologia **17:** 281–291.

Received: 30 July 2004
Accepted: 18 April 2005
Amended: 10 May 2005